NeuroImage 62 (2012) 1469–1477

Contents lists available at SciVerse ScienceDirect

NeuroImage

journal homepage: www.elsevier.com/locate/ynimg

Co-modulatory spectral changes in independent brain processes are correlated with task performance

Shang-Wen Chuang [a,b], Li-Wei Ko [a,c], Yuan-Pin Lin [a], Ruey-Song Huang [a,d], Tzyy-Ping Jung [a,d,e,*], Chin-Teng Lin [a,b,**]

[a] Brain Research Center, University System of Taiwan, Hsinchu, Taiwan
[b] Department of Electrical Engineering, National Chiao-Tung University, Hsinchu, Taiwan
[c] Department of Biological Science and Technology, National Chiao-Tung University, Hsinchu, Taiwan
[d] Swartz Center for Computational Neuroscience, Institute for Neural Computation, University of California, San Diego, CA, USA
[e] Center for Advanced Neurological Engineering, Institute of Engineering in Medicine, University of California, San Diego, CA, USA

ARTICLE INFO

Article history:
Accepted 14 May 2012
Available online 24 May 2012

Keywords:
EEG
Driving
Drowsiness
Independent component analysis (ICA)
Neuromodulatory system
Brain process

ABSTRACT

This study investigates the independent modulators that mediate the power spectra of electrophysiological processes, measured by electroencephalogram (EEG), in a sustained-attention experiment. EEG and behavioral data were collected during 1–2 hour virtual-reality based driving experiments in which subjects were instructed to maintain their cruising position and compensate for randomly induced drift using the steering wheel. Independent component analysis (ICA) applied to 30-channel EEG data separated the recorded EEG signals into a sum of maximally temporally independent components (ICs) for each of 30 subjects. Logarithmic spectra of resultant IC activities were then decomposed by principal component analysis, followed by ICA, to find spectrally fixed and temporally independent modulators (IM). Across subjects, the spectral ICA consistently found four performance-related independent modulators: delta, delta–theta, alpha, and beta modulators that multiplicatively affected the spectra of spatially distinct IC processes when the participants experienced waves of alternating alertness and drowsiness during long-hour simulated driving. The activation of the delta–theta modulator increased monotonically as subjects' task performances decreased. Furthermore, the time courses of the theta–beta modulator were highly correlated with concurrent changes in driving errors across subjects ($r = 0.77 \pm 0.13$).

Introduction

Studies assessing physiological and neural systems across the human alertness–drowsiness dimension have made good progress in the past decades (Cantero et al., 2002, 2004; Kaminski et al., 1997; Oken et al., 2006). The motivation of these studies has mainly been to understand the physiological mechanisms associated with performance declines in attention-demanding tasks in operational, surveillance, or driving environments. Several studies have demonstrated the neuronal correlates of arousal states and sustained attention with invasive assessments (Akimoto et al., 1956; Destexhe et al., 2007; McCormick and Bal, 1997; Steriade, 2000) and non-invasively recorded electroencephalograms (EEG) (Achermann and Borbely, 1998; Beatty et al., 1974; Campagne et al., 2004; Cantero et al., 2002; Duckrow and Zaveri, 2005; Jung et al., 1997; Lin et al., 2005a; Makeig and Inlow, 1993; Makeig and Jung, 1995; Schier, 2000; Takahashi et al., 1997). Scalp EEG measurement has recently gained increasing attention because of its accessibility and potential for real-world applications.

Several studies have demonstrated the use of scalp EEG spectral dynamics as a means for exploring the neurophysiological correlates of human performance and alertness levels. For example, Makeig and Jung (1995) reported that theta- and alpha-power increases during periods of poor task performance. These performance-related spectral changes occur mainly at parietal and occipital regions (Beatty et al., 1974; Campagne et al., 2004; Jung et al., 1997; Lin et al., 2005a), although a few have reported at frontal and central regions (Schier, 2000; Takahashi et al., 1997). Morison and Bassett (1945) also reported that multiple neural mechanisms that affect the transition between arousal and sleep states exhibit distinct spectral fluctuations in the delta, theta, alpha, and beta bands (Morison and Bassett, 1945). The widespread spectral changes over the scalp might be attributable to the fact that scalp EEG signals sum source activities arising within multiple cortical domains that project, by volume conduction, to nearly all the scalp electrodes (Makeig et al., 1996). This signal-mixing process makes it difficult to relate the distinct EEG patterns that originate in

* Correspondence to: T.-P. Jung, Swartz Center for Computational Neuroscience, Institute for Neural Computation, University of California San Diego, 9500 Gilman Dr. #0559, La Jolla, CA 92093-0559, USA. Fax: +1 858 822 7556.
** Correspondence to: C.-T. Lin, CS/EE Departments, National Chiao-Tung University (NCTU), 1001 Ta-Hsueh Road, Hsinchu, 300, Taiwan. Fax: +886 3 572 6272.
E-mail addresses: jung@sccn.ucsd.edu (T-P. Jung), ctlin@mail.nctu.edu.tw (C-T. Lin).

1053-8119/$ – see front matter © 2012 Elsevier Inc. All rights reserved.
doi:10.1016/j.neuroimage.2012.05.035

specific cortical areas to behavior, cognitive functions or pathology, or to identify the origins of distinct EEG sources (Jung et al., 1998, 2001b; Makeig et al., 1996).

Recently, independent component analysis (ICA) applied to multi-channel EEG has proven useful for separating the independent brain and non-brain contributions to the recorded mixtures; this, in turn, has been useful for the analysis of event-related brain temporal activity dynamics during human cognitive tasks (Jung et al., 1998, 2001b; Makeig et al., 1996). Several studies have used ICA to assess the independent components (brain processes) associated with fluctuations in task performance during sustained attention tasks (Huang et al., 2005, 2007a,b, 2008, 2009). In particular, independent components (ICs) with equivalent dipole sources located in the occipital and parietal cortices exhibit tonic increases in theta and alpha band power during high-error periods. It is worth noting that these components are maximally "temporally" independent brain processes, yet they exhibit co-modulatory (dependent) changes in spectral activities that co-vary with performance fluctuation. For example, theta-power increases in most of the independent component activities as task performance declines (Chuang et al., 2009; Huang et al., 2008; Lin et al., 2008). However, the underlying neuromodulatory mechanisms that concurrently mediate these tonic changes in power spectra across multiple independent components were still not understood.

To investigate the physiological and neural modulatory system from alertness to drowsiness, this study proposes a new technique, independent modulator decomposition, to assess co-modulators in the brain during the alertness–drowsiness dimension. The basic hypothesis and principle of using independent modulator decomposition was previously described in Onton and Makeig (2009). The first ICA was applied on multi-channel EEG data to separate the recorded signals into a sum of maximally temporally independent components (ICs). The study further hypothesized that the processes of these underlying neuromodulatory systems vary along with performance fluctuation and are accompanied with the spectral contents of different brain areas. In this spectral decomposition method, the second ICA detected and modeled independent co-modulatory systems that multiplicatively affect the activities of spatially distinct IC processes.

To test these hypotheses, this study explored (1) the co-modulatory (coherent) changes the in spectra of temporally independent components across subjects and (2) the associations between the time courses of the underlying neuromodulatory systems and fluctuations performance of sustained-attention highway-driving tasks conducted in a realistic driving platform.

Materials and methods

Subjects

Thirty right-handed healthy subjects (28 males, 2 females; age range: 18–28 years; age mean and standard deviation: 24 ± 2 years) with normal or corrected to normal vision were paid to participate in a driving experiment. All experiments were conducted in the early afternoon, after lunch, because drowsiness frequently occurs after meals (Benton and Parker, 1998). No subjects reported sleep deprivation the night before the experiment or a history of drug or alcohol abuse. All subjects gave informed consent, and the study was approved by the Institutional Review Broad of the Taipei Veterans General Hospital.

Experimental paradigm

This study adapted an event-related lane-departure driving paradigm originally proposed by Huang et al. (2005, 2007a,b, 2009) in which subjects were instructed to maintain their cruising position and compensate for randomly induced vehicle deviations using the steering wheel. The simulated driving experiments were conducted in a realistic driving simulator (Huang et al., 2005, 2007a,b, 2009; Lin et al., 2005b, 2008, 2011) consisting of a real vehicle mounted on a motion platform with 6 degrees of freedom immersed in a 360-degree virtual-reality (VR) scene. The VR scene included four lanes from left to right on the road. The distance from the left side to the right side of the road is evenly divided into 256 units (digitized into values 0–255). The width of each lane is 60 U. The width of the car is 32 U. To induce drowsiness in the subjects during the driving experiments, the VR scenes simulated monotonous driving at a fixed speed (100 km/h) on a straight and empty highway. Lane-departure events that caused a drift at a constant speed towards the curb or into the opposite lane with equal probability were introduced every 5–10 s, (Huang et al., 2005, 2007a,b, 2009). Without a prompt response from the subject, the vehicle would hit the virtual boundary on either side of the road but would continue to move forward against the boundary without crashing. Subjects were instructed to immediately use the steering wheel to steer the vehicle back to the original cruising position whenever a lane-departure event occurred. To assess driver's drowsiness level by measuring second- or minute-scale fluctuations in driving errors, this study adopted the driving error moving average (DEMA; ranging between 0 and 85 U) as a quantitative behavioral index of drowsiness level (Huang et al., 2009). The DEMA computes the moving average of absolute deviation from the lane in 90-s window stepping at 2-s time intervals. The lower DEMA values are indicated as optimal driving performance and vigilance, whereas higher DEMA values are taken to represent subject drowsiness.

EEG data acquisition and preprocessing

A 32-channel EEG system (Neuroscan, Compumedics Ltd., Australia) was used to record EEGs in the VR-based driving experiments. Scalp electrodes were placed according to the modified International 10–20 system and referred to the linked mastoids (average of channel A1 and channel A2). The impedances of all electrodes were kept below 5 kΩ. The EEG data were sampled at 500 Hz with a 16-bit quantization. A one-channel 8-bit digital event code representing the lane position during the VR-driving simulation was recorded simultaneously. In almost every session of the VR-driving experiments, the subjects' head/arms/body movements during compensatory steering and yawns during drowsy periods were sometimes accompanied by severe, i.e., high-amplitude, artifacts across all channels. These obvious motion artifacts, along with data from bad channels were excluded from further analysis based on visual inspection. A band-pass filter (1–50 Hz) was subsequently applied to EEG data to remove high-frequency muscle artifacts, line-noise contamination and DC drift due to breathing artifacts. After digital filtering, EEG signals and event codes were down-sampled to 250 Hz.

ICA decomposition of multi-channel EEG data

We used an Infomax ICA algorithm (Bell and Sejnowski, 1995; Makeig et al., 1996, 1997) implemented in the EEGLAB toolbox (Delorme and Makeig, 2004) to decompose multi-channel continuous EEG data into maximally temporally independent components based on the assumption that scalp EEG signals are a weighted linear mixture of electrical potentials projected instantaneously from distinct independent brain sources (Bell and Sejnowski, 1995; Makeig et al., 1996, 1997). ICA is capable of deriving an 'unmixing' matrix $\boldsymbol{W}$ that linearly separates $\boldsymbol{N}$-channel EEG signals $\boldsymbol{X}$ into an independent component activation matrix $\boldsymbol{U}$ ($\boldsymbol{U} = \boldsymbol{WX}$). The rows of estimated $\boldsymbol{U}$ are the time courses of the independent component activations. For each subject, ~30 ICs were separated from ~30 channels of EEG (2 EOG channels were excluded) after the training of the ICA unmixing matrix $\boldsymbol{W}$ converged (i.e., weight changes fell below 10^{-6}). The columns of the inverse unmixing matrix $\boldsymbol{W}^{-1}$ represent the relative strength projected from each IC onto each scalp position, which enabled the formation of a color-coded scalp map. Given a scalp map of ICs, the brain source can be further localized with the DIPFIT2 routine (a plug-in for EEGLAB)

to find the 3D location of an equivalent dipole based on a four-shell spherical head model (Oostenveld and Oostendorp, 2002). ICs with a residual variance of dipole fitting to the scalp map that exceeded 15% were excluded from further analysis (Onton and Makeig, 2009). The estimated dipole locations were co-registered with an average brain model (Montreal Neurological Institute). This study assumed that the unmixing matrix $\boldsymbol{W}$ and the dipole source locations of the ICs were fixed regardless of alertness level during each session. To examine the spectral characteristics of the ICs, activation time courses segmented into 3-s (750-point) moving epochs were subjected to fast Fourier transform (FFT), yielding a time series $\boldsymbol{t}$ of logarithmic power spectra with 20 frequency bins $\boldsymbol{f}$ (1–20 Hz) with a stepping time interval of 2-s (500-points) and a frequency resolution near 1 Hz.

Independent component clustering

The consistency of ICs across subjects engaged in VR-driving tasks was assessed by the *K*-means clustering method and visual inspection to semi-automatically group comparable components into distinct clusters based on their scalp maps, power spectra and dipole source locations (Huang et al., 2008; Jung et al., 2001a; Makeig et al., 2002, 2004, 2006). *K*-means was used to derive clusters with greatest distinction by minimizing variability within and maximizing variability between clusters. To make sure the clusters obtained by *K*-means method was optimized, the clustering procedure were repeated 5 times, each with a new set of initial centroids. The resultant component clusters were quite stable across multiple tests. Among the resultant ICA clusters, several clusters account for EEG artifacts (such as eye blinks, eye movements and scalp muscle activity) that are commonly assumed to be functionally independent of cortical source activation (Jung et al., 2001a,b; Makeig et al., 1996, 1997, 2002). The contamination from these non-cortical components could be effectively separated from other EEG processes using ICA. The cortical sources of interest included independent components with equivalent dipole sources located in the frontal medial, central medial, left and right somatomotor, medial parietal, posterior–medial occipital, and bilateral occipital cortices. For each subject, these selected components were further analyzed by independent modulator decomposition (see below) to assess the co-modulatory activities among ICs.

Independent modulator decomposition

To assess the underlying neuromodulator and explore the potential neuromodulator systems that are engaged in human sustained attention, this study adopted the independent modulator analysis (Onton and Makeig, 2009). This analysis is capable of revealing spectrally fixed and temporally independent modulator (IM) processes. The independent modulator analysis was applied to segregate logarithmic spectral fluctuations of independent components of interest into independent modulators, enabling us to summarize the coherent spectral dynamics across one or multiple ICs. For each subject, the mean log-power spectra at each frequency bin, $\boldsymbol{f}$, were subtracted from the logarithmic power spectra of each 3-s epoch of the time series prior to IM decomposition. The baseline-corrected spectral time series (1–30 Hz) of selected ICs were then concatenated to form a 2D matrix ($\boldsymbol{f}\times\boldsymbol{c}$, $\boldsymbol{t}$, where $\boldsymbol{c}$ and $\boldsymbol{t}$ represent the number of selected ICs and time points, respectively). This matrix was submitted to principal component analysis (PCA) that maintained the 10 principal components accounting for the largest variance in spectral changes and yielded a matrix $\boldsymbol{S}$ (10, $\boldsymbol{t}$). The Infomax ICA algorithm (Bell and Sejnowski, 1995; Makeig et al., 1997) was again used to find an unmixing matrix $\boldsymbol{W}$ that linearly separated the dimension-reduced matrix $\boldsymbol{S}$ into maximally spectrally fixed and temporally independent modulators $\boldsymbol{U}$ ($\boldsymbol{U}=\boldsymbol{W}\mathrm{S}$). The rows of $\boldsymbol{U}$ represent the IM activations across time point $\boldsymbol{t}$. Analogous to the inverse unmixing matrix $\boldsymbol{W}^{-1}$ of the first ICA decomposition yielding the column-wise projection strengths of each IC, the columns of $\boldsymbol{W}^{-1}$ of the second ICA represent the relative projection weights from each independent modulator at each frequency bin $\boldsymbol{f}$ across multiple ICs, $\boldsymbol{c}$. The same procedures mentioned for the first ICA decomposition were adopted to train the unmixing matrix $\boldsymbol{W}$. Upon the completion of IM decomposition, the association between driving performance level and the IM of interest was assessed by correlating the IM activations with the 90-s DEMA index separately for each subject.

DEMA-sorted independent modulator activation

To investigate the relationship between fluctuations in task performance and concurrent changes in the activations of independent modulators, we first computed the mean activation of each modulator during "alert" (low DEMA) epochs in each session then computed the difference between the modulators' activations at each time point and the mean "alert" activation for that session. Because modulators' activations were linear combinations of the log spectra of ICs, the modulators' activations resembled log spectra. Therefore, for each modulator, we sorted the activation ratios by task performance (i.e., DEMA) and smoothed the sorted data from each subject. The sorted IM activations at each DEMA level were then averaged across subjects.

Results

Driving performance-related independent components

For each subject, 30 maximally temporally independent components that contained cortical sources, non-cortical artifacts and other mixtures of lower energy sources were separated from the 30-channel EEG data. Non-cortical sources such as eye blinks, eye movements, muscle artifacts, and meaningless components were identified based on the characteristics of their scalp maps, spectra, and dipole locations and removed from further analysis. Only the brain components activated in or near the medial–frontal, medial–parietal, and occipital cortex are addressed and discussed here, as these components have most frequently associated with the driving task (Huang et al., 2005, 2007a,b, 2009). The spectral changes of the aforementioned components were correlated with driving performance fluctuations. After ICA decomposition across all subjects, semi-automatic K-mean clustering based on IC scalp maps, spectra, and dipole locations revealed that the ICs located at the medial–frontal (contributed by 28 subjects), medial–parietal (24 subjects), and occipital (30 subjects) cortices were the three most consistent brain processes across subjects. In addition, all subjects generally experienced several transitions between alertness and drowsiness during the VR-based driving experiments as evidenced by the DEMA measures.

Fig. 1 shows sample delta-, theta-, alpha-, and beta-band spectral time courses of three ICs of interest and the corresponding simultaneous DEMA time course from a single subject. The DEMA index and spectral time series were smoothed with a 90-s window stepping at 2-s time intervals. Figs. 1(b) and (c) clearly show that the time courses of the delta and theta power of all three components were highly correlated with each other and co-varied with the subject's DEMA ($r=0.91$–0.93 for the delta power; $r=0.89$–0.93 for theta power). The alpha-band power time courses of the medial–parietal and occipital components (Fig. 1(d)) were moderately correlated with driving performance ($r=0.63$–0.66), whereas the time courses of beta-band power of all components (Fig. 1(e)) marginally co-varied with driving performance ($r=0.51$–0.87). The mean activation of alpha-band power similarly increased as DEMA increased but gradually decreased during periods of high DEMA levels. These results show that, although different components represented maximally "temporally" independent brain processes, they exhibited co-modulatory (dependent) changes in spectral activities that co-vary with performance fluctuation. The subsequent analysis examines these co-modulatory spectral changes arising from the medial–frontal, medial–parietal, and occipital cortices.

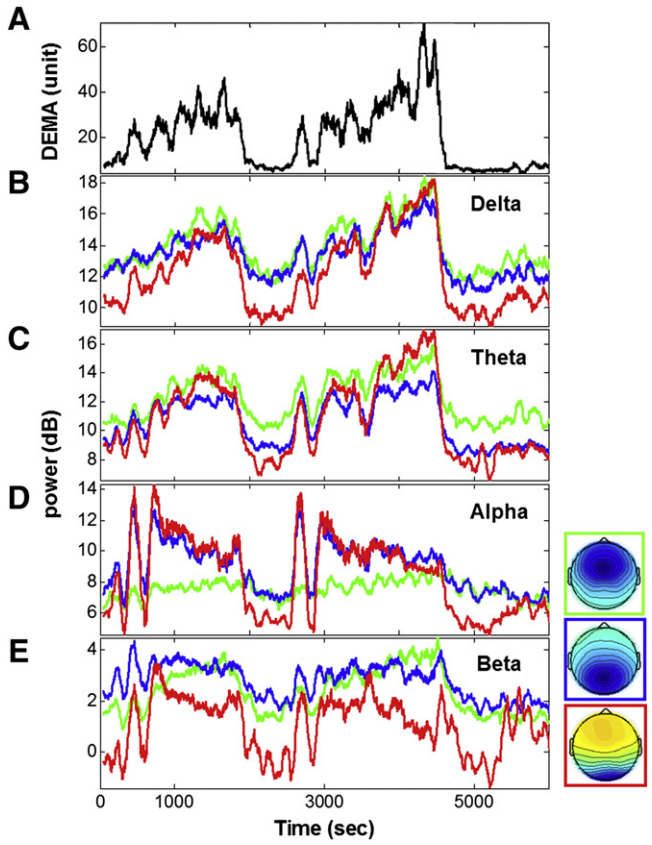

Fig. 1. Fluctuations of task performance (driving error moving average) and power spectra changes of three selected independent components (subject 1) during a 2-hour lane-keeping driving task. (A) Time series of the driving error moving average (DEMA). (B) Time series of delta-band power. (C) Time series of theta-band power. (D) Time series of alpha-band power. (E) Time series of beta-band power.

Selection of independent modulators and components

The logarithmic spectral fluctuations from physiologically interpretable brain sources were further subjected to IM decomposition forming a 2D matrix ($f \times c$, t). Note that the number of cortical components can vary across subjects because each individual may engage distinct brain processes during the driving task (Jung et al., 2001a). IM decomposition was applied to a PCA-reduced matrix that retained the first 10 principal components for each subject. Fig. 2 shows a representative single-subject independent modulation decomposition of log power of activations of temporally independent components in the VR-based driving experiment. Each column represents one IM that gives the relative projection weights to each frequency bin of each IC (along rows). We propose a quantitative index to assess the relationship between the modulators and task performance. For each subject, the averaged weights of the delta, theta, alpha and beta bands were firstly computed to assess the type of each independent modulator. By calculating the correlation between the time courses of each modulator and driving performance (i.e., DEMA) for each individual, the most strongly correlated independent modulator from each band was obtained for further investigation. For this subject, the time courses of four IMs (IM8, IM2, IM1, and IM6) were consistently correlated with DEMA fluctuations ($r = 0.32$, 0.90, 0.30, and 0.10, respectively). IM8, IM2, IM1, and IM6 showed relatively dominant projection weights in the delta, delta–theta, alpha, and beta bands across multiple ICs. Note that each of the IMs modulated the spectral changes of multiple brain regions delineated by ICs.

Consistency of independent modulators across subjects

To access the consistency of the IMs of interest across subjects, Fig. 3 plots the projection strengths of delta, delta–theta, alpha and beta modulators over the medial–frontal, medial–parietal, and occipital ICs. The leftmost two columns show the averaged scalp maps and individual dipole locations within an IC cluster (along rows), whereas the rightmost four columns plot the individual (thin line) and averaged (thick line) weights of each frequency bin (1–30 Hz) of each independent brain process to each IM derived from the column of the inverse matrix $\boldsymbol{W}^{-1}$ at IM decomposition. The spectral weights of ICs largely define the frequency bins at which the ICs' spectra were modulated by the IM during the simulated driving experiments. Note that the spectral weights of each IM were normalized across subjects in Fig. 3. As Fig. 3 shows, the spectral weights of these selected IMs are extremely similar across subjects (thin lines), which was quite remarkable considering the independent modulation decomposition was applied to the log-power ICs of each individual separately. The subject variability was evident in Table 1. Most of the subjects showed high correlations between IMs and the performances in the delta–theta IM, but subjects 2, 13, 14, 15, 20, 21, 25, and 28 showed comparable correlations in the delta–theta IM and the alpha IM, and subject 17 had the highest correlation in the alpha IM.

Relationship between modulators' activations and task performance

This study further tests the neurophysiological meaning of the activations of IMs during the simulated driving task. Fig. 4 plots the DEMA and activation time courses of four IMs from a sample subject. As Fig. 4 shows, the activation of the delta–theta modulator was highly correlated with the subject's DEMA profile ($r = 0.9$), whereas the delta-, alpha-, and beta-modulated activations were only moderately correlated with the DEMA (delta: $r = 0.32$, alpha: $r = 0.30$, and beta: $r = 0.30$). Specifically, the time course of the alpha modulator prominently decreased at high DEMA levels, in contrast to the delta–theta IM activity. As scale and polarity information is distributed in the ICA decomposition, the absolute amplitude and polarity of the modulatory activity are meaningless and the activations have no unit of measure. The scale of the time course of the modulatory activity uses arbitrary units. Table 1 shows the correlation coefficients between the task-related independent modulators and the performance of each individual. Across subjects, four IMs, the delta, delta–theta, alpha, and beta band activations of ICs, were found to consistently correlate with DEMA fluctuations ($r = 0.23 \pm 0.17$, 0.77 ± 0.13, 0.50 ± 0.20, and 0.32 ± 0.18, respectively).

Group DEMA-related modulator fluctuations

To evaluate the inter-subject variability of the IM activations engaged during driving performance, the IM activations were first sorted by subjective ascending DEMA level for each subject, and then the sorted IM activations at each DEMA level were averaged across subjects (cf. Materials and methods).

Fig. 5 shows the averaged DEMA-sorted activations of the aforementioned delta, delta–theta, alpha, and beta modulators across 30 subjects. The results in Fig. 5 clearly indicate that the mean activations of the delta–theta modulator increased monotonically with DEMA values with a high correlation of 0.77 ± 0.13. The mean activation of the alpha modulator similarly increased as DEMA increased, but it gradually reached a plateau above a DEMA level of 20, followed by a slight decline after DEMA reached 60. This biphasic change resulted in a moderate correlation between the modulator's activation and DEMA values ($r = 0.50 \pm 0.20$). Similarly, the activations of the delta and beta modulators tended to increase before DEMA values reached 20 and then declined after DEMA values passed 60. The delta and beta modulators had marginal correlations with DEMA values (delta: $r = 0.23 \pm 0.17$, beta: $r = 0.32 \pm 0.18$).

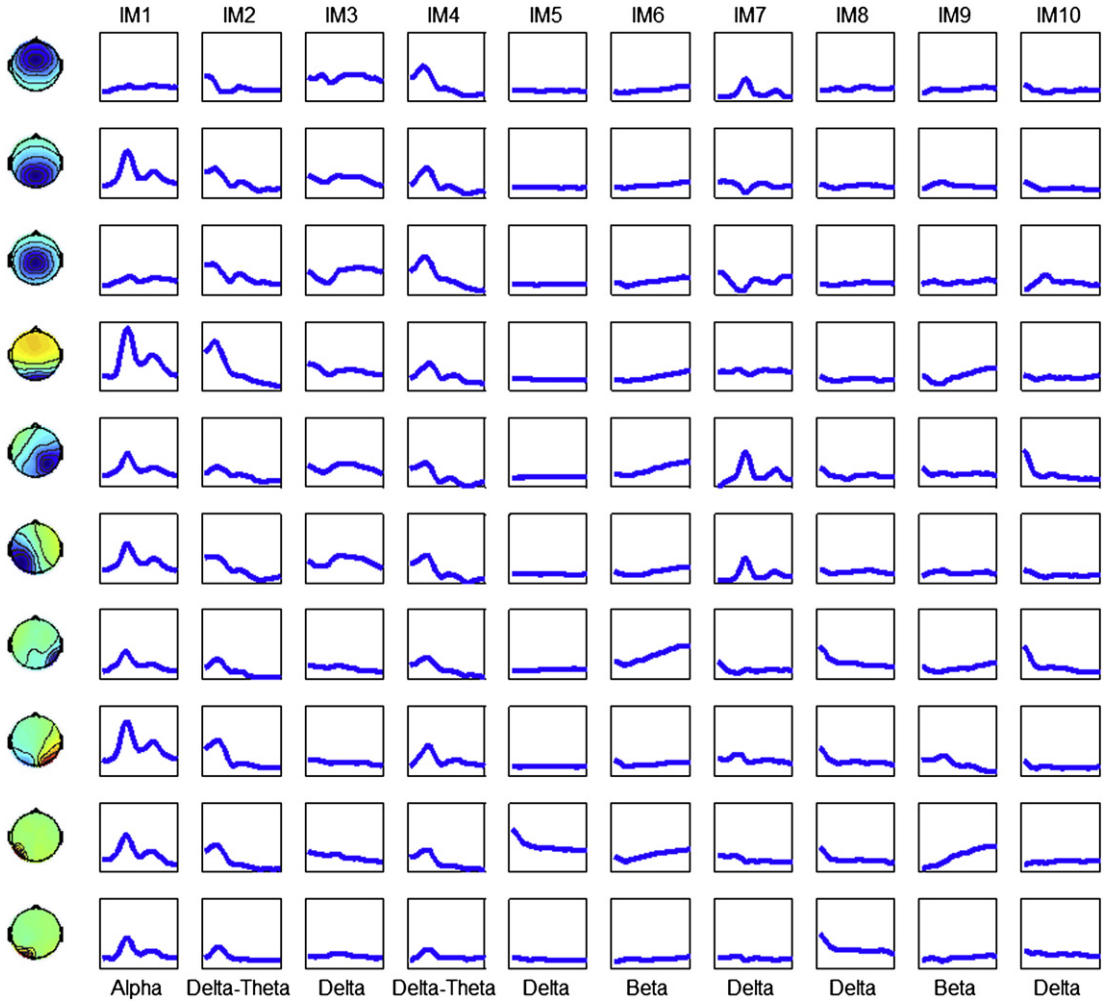

Fig. 2. Independent modulator decomposition log-spectral power results from one representative subject in a VR-based driving experiment. Each column represents one IM and gives the relative projection weights to each frequency of each IC (along rows). In this subject IM8, IM2, IM1, and IM6 show dominate projection weights at delta, delta–theta, alpha, and beta bands across multiple ICs. The IM2 obviously co-modulated the delta–theta band power changes across all ICs, as evidenced by the consistent projection weight with dominate peaks at the delta–theta band. In each sub-figure, the x-axis means the frequency bins from 0 to 30 Hz, and the y-axis means the relative projection weights from 0 to 2.

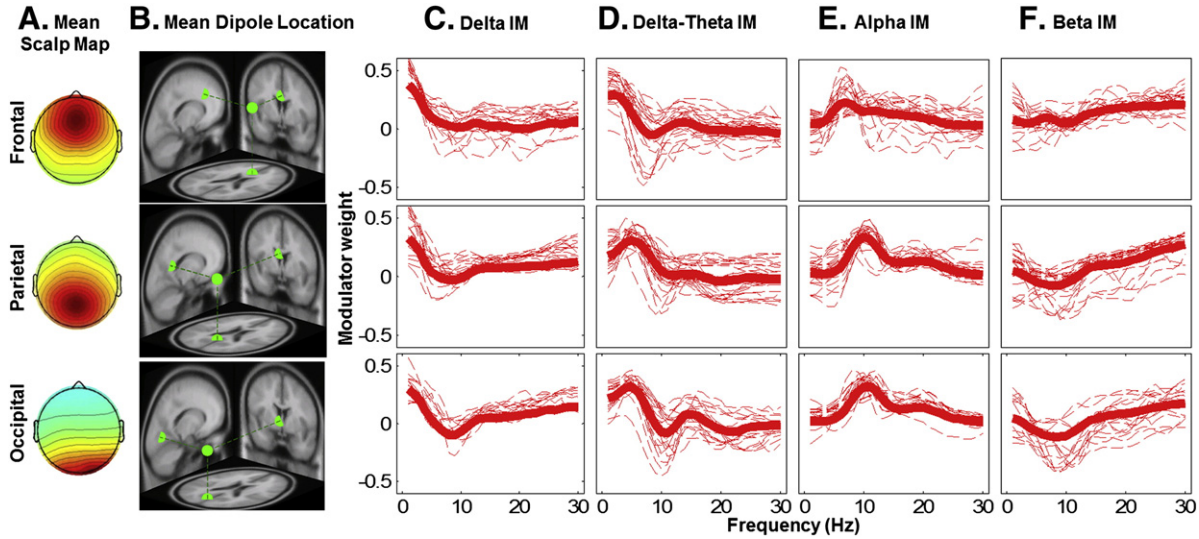

Fig. 3. Normalized spectral weights of delta, delta–theta, alpha and beta modulators over the medial–frontal, medial–parietal, and occipital ICs among 30 subjects. The leftmost two columns show the averaged scalp map and dipole location within an IC cluster (along rows). The rightmost four columns show the individual (thin line) and averaged (thick line) projection weights from each IM to each frequency (1–30 Hz) of each independent brain process, derived from the column of the inverse matrix $\boldsymbol{W}^{-1}$ of IM decomposition. It clearly indicates that four modulators revealed a prominent delta, delta–theta, alpha, and beta peak over three areas consistently across subjects. Note that the projected spectral weights of each IM were normalized across subjects.

Table 1
The correlation coefficients between the task-related independent modulators and the performance of each individual.

Subject	Correlation coefficients between IMs and the performance			
	Delta IM	Delta–theta IM	Alpha IM	Beta IM
1	0.18	0.88	0.2	0.38
2	0.46	0.65	0.66	0.59
3	0.58	0.77	0.25	0.29
4	0.3	0.93	0.2	0.27
5	0.36	0.65	0.48	0.47
6	0.38	0.8	0.48	0.13
7	0.34	0.83	0.69	0.58
8	0.22	0.78	0.28	0.49
9	0.1	0.77	0.57	0.43
10	0.02	0.85	0.44	0.12
11	0.28	0.74	0.14	0.66
12	0.11	0.76	0.56	0.23
13	0.28	0.79	0.73	0.09
14	0.1	0.65	0.64	0.12
15	0.08	0.71	0.76	0.17
16	0.08	0.77	0.28	0.11
17	0.14	0.37	0.86	0.52
18	0.06	0.85	0.75	0.14
19	0.09	0.84	0.51	0.15
20	0.2	0.71	0.75	0.09
21	0.19	0.44	0.38	0.12
22	0.11	0.73	0.49	0.26
23	0.04	0.93	0.63	0.24
24	0.19	0.95	0.47	0.37
25	0.18	0.68	0.63	0.51
26	0.03	0.89	0.55	0.55
27	0.55	0.88	0.37	0.44
28	0.37	0.79	0.77	0.27
29	0.63	0.81	0.24	0.63
30	0.32	0.9	0.3	0.3
Mean	0.23	0.77	0.50	0.32
SD	0.17	0.13	0.20	0.18
Max	0.63	0.95	0.86	0.66
Min	0.02	0.37	0.14	0.09

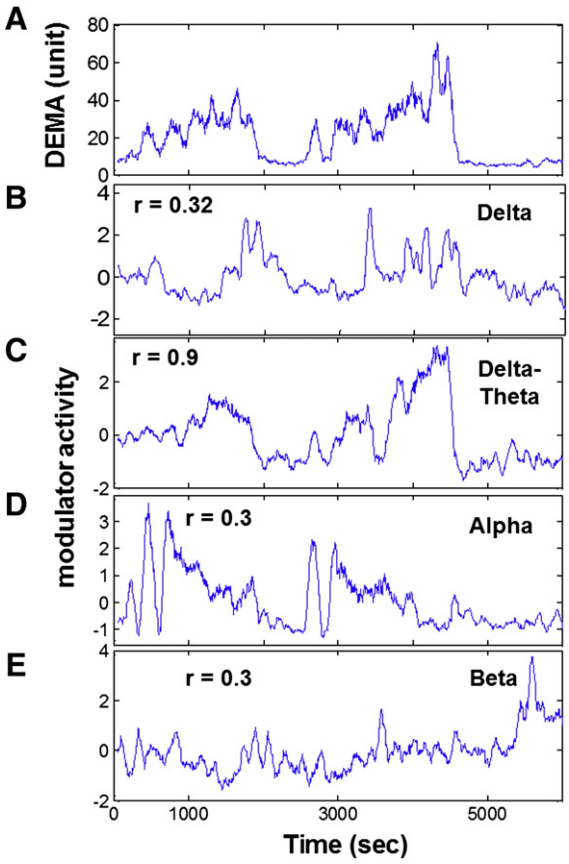

Fig. 4. One representative single-subject's activation time courses of four IMs accompanied by simultaneous DEMA time courses. The activation of the delta–theta modulator was highly correlated with the subject's DEMA profile ($r = 0.9$), whereas the delta-, alpha-, and beta-modulated activations only moderately co-varied with DEMA (delta: $r = 0.32$, alpha: $r = 0.30$, and beta: $r = 0.30$). Specifically, the time course of the alpha modulator prominently decreased as DEMA increased, in contrast to delta–theta IM activity. The correlation coefficients are marked at each subject's modulator activation.

Discussion

Driving performance-related independent components

The time courses of the delta, theta, alpha and beta power spectra of several brain regions, as identified with spatial filters learned from ICA, were highly correlated with each other. Compatible with earlier findings in different sustained-attention tasks, delta-band power increased as task performance declined (Kirmizi-Alsan et al., 2006; Torsvall and aAkerstedt, 1987; Uchida et al., 1991), and the theta-band power of several brain regions was highly correlated with task performance changes (Akerstedt and Gillberg, 1990; Beatty et al., 1974; Campagne et al., 2004; Jung et al., 1997; Kecklund and Akerstedt, 1993; Lal and Craig, 2002; Makeig and Jung, 1995, 1996; Makeig et al., 2000; Takahashi et al., 1997).

Consistent with earlier findings, alpha-band power increased as the DEMA increased from near-perfect performance (Akerstedt and Gillberg, 1990; Huang et al., 2009; Makeig and Jung, 1995, 1996; Makeig et al., 2000; Schier, 2000). Moreover, the alpha band power decreased as the DEMA continued to increase, consistent with the biphasic trend along the human alertness–drowsiness dimension reported by Ota et al. (1996).

As shown in Fig. 5, the averaged DEMA-sorted activation strength of the delta, delta–theta, alpha, and beta modulators across 30 subjects all increased from alert to drowsy states. These results were consistent with Lal and Craig. (2002) that reported a broad-band low-frequency power increase as subjects became fatigued. However, this study provided new insights into the covariation of spectral changes of distinct EEG sources as a function of performance degradation, which were not available in previous studies.

Driving performance-related independent modulators

The present study proposes a new method to assess co-modulatory spectral changes among multiple brain regions during a sustained-attention task. We applied PCA and a second ICA to normalized log spectral changes of independent components to separate independent modulators for each participant. Across subjects, this spectral ICA consistently found four comparable (common) performance-related independent modulators: delta, delta–theta, alpha, and beta modulators. Although the independent modulator decomposition was applied to the components' log spectra for each subject separately, the spectral weights of comparable IMs were remarkably similar across subjects (c.f. thin traces in Fig. 3). Furthermore, the relationship between the activations of these common modulators and task performance was very consistent across subjects (detailed below).

The amplitude of the delta–theta modulator increased monotonically with DEMA values (cf. Figs. 4 and 5B). Previous research has demonstrated that delta waves in the normal adult are largest during deep sleep, and theta rhythm is the EEG characteristic of sleep stage 1 and microsleep. (Bear et al., 2007; De Gennaro et al., 2001; Thomas et al., 2003).

The alpha modulator was very sensitive to performance changes, particularly from fully alert (low DEMA) to high DEMA periods (c.f. Figs. 4 and 5C). The modulator amplitude rose steadily until the DEMA reached 20 after which it remained more or less stable until the DEMA reached 60, and then it started declining slightly at higher DEMAs. Overall, this biphasic trend during the transition from waking to sleeping is consistent

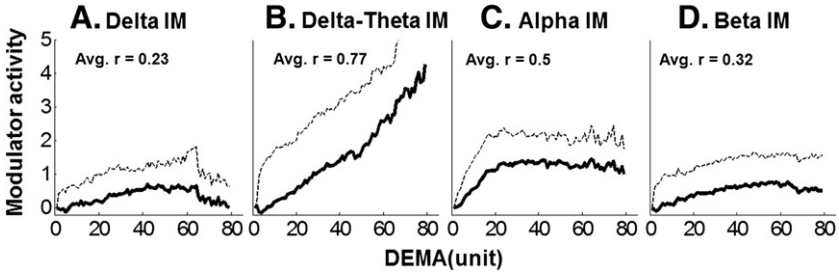

Fig. 5. The averaged DEMA-sorted independent modulator activation strength across 30 subjects. (A) Delta modulator. (B) Delta–theta modulator. (C) Alpha modulator. (D) Beta modulator. Thick and thin traces represent the grand mean and one standard deviation across 30 subjects. The results clearly indicate that the mean activation of the delta–theta modulator increased monotonically as the DEMA increased with a high correlation of 0.77 ± 0.13. The mean activation of the alpha modulator similarly increased as DEMA increased, but it gradually reached a plateau above a DEMA level of 20, followed by a decline after DEMA reached 60. Note that the full width of each lane is 60 units.

with previous studies (Ogilvie, 2001; Ota et al., 1996). Past literature has demonstrated that alpha band power increases are an electrophysiological characteristic correlated with cortical idling (Goldman et al., 2002; Laufs et al., 2003; Pfurtscheller and Stancak, 1996) and are decreased by temporal attention (Babiloni et al., 2004; Bastiaansen et al., 2001). Therefore, the increased alpha-band power of the frontal, parietal and occipital lobes in this study might be partially attributed to cortical idling or decreased attentiveness during the transition from perfect driving performance to medium DEMAs. Changes in the delta and beta modulators marginally fluctuated with task performance (c.f. Figs. 4, 5A and D). Eoh et al. (2005) reported that beta rhythm decreases when subjects are drowsy.

The modulatory mechanisms of the neural system

There are multiple neuromodulatory mechanisms mediating activations of different brain networks in various arousal states (Oken et al., 2006). This study assessed the influence of these multiple neural mechanisms that are observed in the modulation of spectral contents of different brain areas.

This interareal co-modulation may be attributed to the influence of cortical and thalamic projections (Akimoto et al., 1956; Bardo, 1998; McCormick and Bal, 1997; Oken et al., 2006; Robbins, 1997). A cortico-thalamocortical network involves thalamus receiving input from one cortical area and projecting to a higher-order cortical area (Sherman and Guillery, 1996, 2006). Studies have reported that thalamo-cortical networks strongly affect the spectral synchronization of cortical field potentials (Herculano-Houzel et al., 1999; Pinault, 1992; Swick et al., 1994). Lopes da Silva (1991) also reported that the thalamo-cortical loops play a significant role in the generation and control of low frequency rhythms in cortical processes. Furthermore, studies using simultaneous recording of EEG and functional imaging techniques to investigate the neuromodulatory system have supported the theory of cortical and subcortical modulation of electroencephalographic rhythms. For example, a combined EEG/PET study reported a close functional relationship between subcortical regions and human alpha rhythms mediated by the thalamo-cortical network (Schreckenberger et al., 2004). Feige (2005) applied simultaneous EEG/fMRI recording and found that a widespread thalamo-cortical synchronization was associated with brain metabolic changes accompanied by concurrent changes of the alpha rhythm. We thus believe that the modulation of component spectra might be attributed to the influence of cortical and thalamic projections.

In regards to the spectral contents of co-modulation, the co-modulation in this study was predominately occurred in low frequency. The functional thalamo-cortical activity exhibits two distinct states: (a) the burst state which is characterized by synchronized rhythmic delta, spindle, and slow-wave activity during slow wave sleep (McCarley et al., 1983; McCormick and Bal, 1997); and (b) the tonic state which is characterized by less rhythmic, less synchronous, lower amplitude thalamo-cortical activity during waking and rapid-eye-movement sleep (McCormick and Bal, 1997; Steriade, 2000).

The modulation of component spectra might also be attributed to reduced cortical effective connectivity. Esser et al. (2009) envisioned that the transition from wakefulness to slow wave sleep would produce a cortical gate through some underlying mechanisms. Massimini et al. (2005) applied transcranial magnetic stimulation (TMS) to evoke activity rapidly propagating to specific cortical areas, and reported that reduced cortical effective connectivity during slow wave sleep could be accounted for by the existence of a cortical gate. The cortical gate acts like a low-pass filter, allowing slow, widespread activity to propagate through the brain, while blocking the propagation of fast fluctuations.

Our experimental results showed that the synchronized fluctuations of theta-band power are comparable between frontal, central–parietal and occipital components, which might reflect a signal from the deep brain projecting to cortical areas. Spatially non-contiguous area that showed covariation of EEG spectral fluctuations might also be caused by the reduction of cortical–cortical connectivity which rendered the cortex more susceptible to subcortical synchronizing influences, or attributed to this thalamo-cortical activity through the thalamic gate (Miller and Schreiner, 2000).

Limitations (feasibility) of the co-modulation analysis

This study investigates the independent modulators, as separated by independent modulator decomposition, that mediate the power of delta, theta, alpha, and beta bands of electrophysiological processes in alertness–drowsiness experiments. However, little is known about the possible physical locations of the resultant independent co-modulators. Another limitation of independent modulator decomposition is that little information about direct or indirect connectivity between ICs was provided by this independent modulatory decomposition. Other converging evidence is needed to assess ICs' functional connectivity. Our future work includes a comparison between linear and non-linear regression between the subject performance and the activations of co-modulators. We also plan to evaluate the feasibility of using the activations of co-modulators to predict/detect the level of drowsiness in an on-line setting.

Conclusion

This study explored spectrally independent modulators derived by the second ICA to investigate the neural mechanisms mediating spectral activations of cortical areas. Across subjects, the analysis consistently obtained four comparable independent modulators that mediated the delta, delta–theta, alpha, and beta power of different brain areas. The delta–theta modulator fluctuated very little during the low DEMA periods, but increased monotonically with DEMA values. More interestingly, the time courses of the delta–theta modulator were highly correlated with concurrent changes in subject driving error (DEMA). The activation of the alpha modulator rose rapidly from a fully alert to medium DEMA state, but decreased at high DEMA states. The time courses of the delta and beta modulators were only moderately correlated with concurrent changes in subject task performance.

Acknowledgments

This work was supported in part by the Aiming for the Top University Plan of National Chiao Tung University, the Ministry of Education, Taiwan, under Contract 100W963, and in part by the UST-UCSD International Center of Excellence in Advanced Bio-engineering sponsored by the Taiwan National Science Council I-RiCE Program under Grant Number: NSC-100-2911-I-009-101. This research was also sponsored in part by Office of Naval Research, Army Research Office (under contract number W911NF-09-1-0510) and Army Research Laboratory (under Cooperative Agreement Number W911NF-10-2-0022). The views and the conclusions contained in this document are those of the authors and should not be interpreted as representing the official policies, either expressed or implied, of the Army Research Laboratory or the U.S Government. The U.S Government is authorized to reproduce and distribute reprints for government purposes notwithstanding any copyright notation herein.

References

Achermann, P., Borbely, A., 1998. Coherence analysis of the human sleep electroencephalogram. Neuroscience 85, 1195–1208.
Akerstedt, T., Gillberg, M., 1990. Subjective and objective sleepiness in the active individual. Int. J. Neurosci. 52, 29–37.
Akimoto, H., Yamaguchi, N., Okabe, K.-i., Nakagawa, T., Nakamura, I., Abe, R., Torii, H., Masahashi, K., 1956. On the sleep induced through electrical stimulation on dog thalamus. Psychiatry Clin. Neurosci. 10, 117–146.
Babiloni, C., Miniussi, C., Babiloni, F., Carducci, F., Cincotti, F., Del Percio, C., Sirello, G., Fracassi, C., Nobre, A.C., Rossini, P.M., 2004. Sub-second. Cogn. Brain Res. 19, 259–268.
Bardo, M., 1998. Neuropharmacological mechanisms of drug reward: beyond dopamine in the nucleus accumbens. Crit. Rev. Neurobiol. 12, 37.
Bastiaansen, M., Bocker, K.B.E., Brunia, C.H.M., de Munck, J.C., Spekreijse, H., 2001. Event-related desynchronization during anticipatory attention for an upcoming stimulus: a comparative EEG/MEG study. Clin. Neurophysiol. 112, 393–403.
Bear, M.F., Connors, B.W., Paradiso, M.A., 2007. Neuroscience: exploring the brain. Lippincott Williams & Wilkins.
Beatty, J., Greenberg, A., Deibler, W.P., O'Hanlon, J.F., 1974. Operant control of occipital theta rhythm affects performance in a radar monitoring task. Science 183, 871–873.
Bell, A.J., Sejnowski, T.J., 1995. An information maximization approach to blind separation and blind deconvolution. Neural Comput. 7, 1129–1159.
Benton, D., Parker, P.Y., 1998. Breakfast, blood glucose, and cognition. Am. J. Clin. Nutr. 67, 772s–778s.
Chuang, S.W., Huang, R.S., Ko, L.W., Jeng, J.L., Duann, J.R., Jung, T.P., Lin, C.T., 2009. Independent modulators mediate spectra of multiple brain processes in a VR-based driving experiment. Proceedings of SPIE, the International Society for Optical Engineering 7343, 73431C.
Campagne, A., Pebayle, T., Muzet, A., 2004. Correlation between driving errors and vigilance level: influence of the driver's age. Physiol. Behav. 80, 515–524.
Cantero, J.L., Atienza, M., Salas, R.M., 2002. Human alpha oscillations in wakefulness, drowsiness period, and REM sleep: different electroencephalographic phenomena within the alpha band. Neurophysiol. Clin. 32, 54–71.
Cantero, J.L., Atienza, M., Madsen, J.R., Stickgold, R., 2004. Gamma EEG dynamics in neocortex and hippocampus during human wakefulness and sleep. Neuroimage 22, 1271–1280.
De Gennaro, L., Ferrara, M., Bertini, M., 2001. The boundary between wakefulness and sleep: quantitative electroencephalographic changes during the sleep onset period. Neuroscience 107, 1–11.
Delorme, A., Makeig, S., 2004. EEGLAB: an open source toolbox for analysis of single-trial EEG dynamics including independent component analysis. J. Neurosci. Methods 134, 9–21.
Destexhe, A., Hughes, S.W., Rudolph, M., Crunelli, V., 2007. Are corticothalamic 'up' states fragments of wakefulness? Trends Neurosci. 30, 334–342.
Duckrow, R., Zaveri, H., 2005. Coherence of the electroencephalogram during the first sleep cycle. Clin. Neurophysiol. 116, 1088–1095.
Eoh, H.J., Chung, M.K., Kim, S.H., 2005. Electroencephalographic study of drowsiness in simulated driving with sleep deprivation. Int. J. Ind. Ergon. 35, 307–320.
Esser, S.K., Hill, S., Tononi, G., 2009. Breakdown of effective connectivity during slow wave sleep: investigating the mechanism underlying a cortical gate using large-scale modeling. J. Neurophysiol. 102 (4), 2096–2111.
Feige, B., Scheffler, K., Esposito, F., Di Salle, F., Hennig, J., Seifritz, E., 2005. Cortical and subcortical correlates of electroencephalographic alpha rhythm modulation. Journal of Neurophysiology 93, 2864–2872.
Goldman, R.I., Stern, J.M., Engel Jr., J., Cohen, M.S., 2002. Simultaneous EEG and fMRI of the alpha rhythm. Neuroreport 13, 2487.
Herculano-Houzel, S., Munk, M.H.J., Neuenschwander, S., Singer, W., 1999. Precisely synchronized oscillatory firing patterns require electroencephalographic activation. J. Neurosci. 19, 3992.
Huang, R.S., Jung, T.P., Makeig, S., 2005. Analyzing event-related brain dynamics in continuous compensatory tracking tasks. 27th Annual International Conference of the Engineering in Medicine and Biology Society, pp. 5750–5753.
Huang, R.S., Jung, T.P., Makeig, S., 2007a. Event-related brain dynamics in continuous sustained-attention tasks. 12th International Conference on Human-Computer Interaction (HCI), pp. 65–74.
Huang, R.S., Jung, T.P., Makeig, S., 2007b. Multi-scale EEG brain dynamics during sustained attention tasks. Proceeding of IEEE International Conference on Acoustics, Speech, and Signal Processing (ICASSP), pp. IV1173–IV1176.
Huang, R.S., Jung, T.P., Delorme, A., Makeig, S., 2008. Tonic and phasic electroencephalographic dynamics during continuous compensatory tracking. Neuroimage 39, 1896–1909.
Huang, R.S., Jung, T.P., Makeig, S., 2009. Tonic changes in EEG power spectra during simulated driving. Lecture Notes in Computer Science, Foundations of Augmented Cognition: Neuroergonomics and Operational Neuroscience, pp. 394–403.
Jung, T.P., Makeig, S., Stensmo, M., Sejnowski, T.J., 1997. Estimating alertness from the EEG power spectrum. IEEE Trans. Biomed. Eng. 44, 60–69.
Jung, T.P., Makeig, S., Bell, A.J., Sejnowski, T.J., 1998. Independent component analysis of electroencephalographic and event-related potential data. Central Auditory Processing and Neural Modeling, pp. 189–197.
Jung, T.P., Makeig, S., McKeown, M.J., Bell, A.J., Lee, T.W., Sejnowski, T.J., 2001a. Imaging brain dynamics using independent component analysis. Proc. IEEE 89, 1107–1122.
Jung, T.P., Makeig, S., Westerfield, M., Townsend, J., Courchesne, E., Sejnowski, T.J., 2001b. Analysis and visualization of single trial event related potentials. Hum. Brain Mapp. 14, 166–185.
Kaminski, M., Blinowska, K., Szelenberger, W., 1997. Topographic analysis of coherence and propagation of EEG activity during sleep and wakefulness. Electroencephalogr. Clin. Neurophysiol. 102, 216–227.
Kecklund, G., Akerstedt, T., 1993. Sleepiness in long distance truck driving: an ambulatory EEG study of night driving. Ergonomics.
Kirmizi-Alsan, E., Bayraktaroglu, Z., Gurvit, H., Keskin, Y.H., Emre, M., Demiralp, T., 2006. Comparative analysis of event-related potentials during Go/NoGo and CPT: decomposition of electrophysiological markers of response inhibition and sustained attention. Brain Res. 1104, 114–128.
Lal, S.K.L., Craig, A., 2002. Driver fatigue: electroencephalography and psychological assessment. Psychophysiology 39, 313–321.
Laufs, H., Kleinschmidt, A., Beyerle, A., Eger, E., Salek-Haddadi, A., Preibisch, C., Krakow, K., 2003. EEG-correlated fMRI of human alpha activity. Neuroimage 19, 1463–1476.
Lin, C.T., Wu, R.C., Jung, T.P., Liang, S.F., Huang, T.Y., 2005a. Estimating driving performance based on EEG spectrum analysis. EURASIP J. Appl. Signal Process. 19, 3165–3174.
Lin, C.T., Wu, R.C., Liang, S.F., Huang, T.Y., Chao, W.H., Chen, Y.J., Jung, T.P., 2005b. EEG-based drowsiness estimation for safety driving using independent component analysis. IEEE Trans. Circ. Syst. 52, 2726–2738.
Lin, C.T., Chen, Y.C., Huang, T.Y., Chiu, T.T., Ko, L.W., Liang, S.F., Hsieh, H.Y., Hsu, S.H., Duann, J.R., 2008. Development of wireless brain computer interface with embedded multitask scheduling and its application on real-time driver's drowsiness detection and warning. IEEE Trans. Biomed. Eng. 55, 1582–1591.
Lin, C.T., Liao, L.D., Liu, Y.H., Wang, I.J., Lin, B.S., Chang, J.Y., 2011. Novel dry polymer foam electrodes for long-term EEG measurement. IEEE Trans. Biomed. Eng. 58, 1200–1207.
Lopes da Silva, F., 1991. Neural mechanisms underlying brain waves: from neural membranes to networks. Electroencephalogr. Clin. Neurophysiol. 79, 81–93.
Makeig, S., Inlow, M., 1993. Lapse in alertness: coherence of fluctuations in performance and EEG spectrum. Electroencephalogr. Clin. Neurophysiol. 86, 23–35.
Makeig, S., Jung, T.P., 1995. Changes in alertness are a principal component of variance in the EEG spectrum. Neuroreport 7, 213–216.
Makeig, S., Jung, T.P., 1996. Tonic, phasic, and transient EEG correlates of auditory awareness in drowsiness. Cogn. Brain Res. 4, 15–25.
Makeig, S., Bell, A.J., Jung, T.P., Sejnowski, T.J., 1996. Independent component analysis of electroencephalographic data. Adv. Neural Inf. Process. Syst. 8 (8), 145–151.
Makeig, S., Jung, T.P., Bell, A.J., Ghahremani, D., Sejnowski, T.J., 1997. Blind separation of auditory event-related brain responses into independent components. Proc. Natl. Acad. Sci. U. S. A. 94, 10979–10984.
Makeig, S., Jung, T.P., Sejnowski, T.J., 2000. Awareness during drowsiness: dynamics and electrophysiological correlates. Can. J. Exp. Psychol. 54, 266.
Makeig, S., Westerfield, M., Jung, T.P., Enghoff, S., Townsend, J., Courchesne, E., Sejnowski, T., 2002. Dynamic brain sources of visual evoked responses. Science 295, 690.
Makeig, S., Delorme, A., Westerfield, M., Jung, T.P., Townsend, J., Courchesne, E., Sejnowski, T.J., 2004. Electroencephalographic brain dynamics following manually responded visual targets. PLoS Biol. 2, 747–762.
Makeig, S., Onton, J., Westerfield, M., Townsend, J., 2006. Imaging human EEG dynamics using independent component analysis. Neurosci. Biobehav. Rev. 30, 808–822.
Massimini, M., Ferrarelli, F., Huber, R., Esser, S.K., Singh, H., Tononi, G., 2005. Breakdown of cortical effective connectivity during sleep. Science 309, 2228–2232.
McCarley, R.W., Benoit, O., Barrionuevo, G., 1983. Lateral geniculate nucleus unitary discharge in sleep and waking: state-and rate-specific aspects. J. Neurophysiol. 50, 798.
McCormick, D.A., Bal, T., 1997. Sleep and arousal: thalamocortical mechanisms. Annu. Rev. Neurosci. 20, 185–215.
Miller, L.M., Schreiner, C.E., 2000. Stimulus-based state control in the thalamocortical system. J. Neurosci. 20, 7011.
Morison, R., Bassett, D., 1945. Electrical activity of the thalamus and basal ganglia in decorticate cats. J. Neurophysiol. 8, 309.
Ogilvie, R.D., 2001. The process of falling asleep. Sleep Med. Rev. 5, 247–270.
Oken, B., Salinsky, M., Elsas, S., 2006. Vigilance, alertness, or sustained attention: physiological basis and measurement. Clin. Neurophysiol. 117, 1885–1901.
Onton, J., Makeig, S., 2009. High-frequency broadband modulations of electroencephalographic spectra. Front. Hum. Neurosci. 3, 61.

Oostenveld, R., Oostendorp, T.F., 2002. Validating the boundary element method for forward and inverse EEG computations in the presence of a hole in the skull. Hum. Brain Mapp. 17, 179–192.
Ota, T., Toyoshima, R., Yamauchi, T., 1996. Measurements by biphasic changes of the alpha band amplitude as indicators of arousal level. Int. J. Psychophysiol. 24, 25–37.
Pfurtscheller, G., Stancak, A., 1996. Event-related synchronization (ERS) in the alpha band—an electrophysiological correlate of cortical idling: a review. Int. J. Psychophysiol. 24, 39–46.
Pinault, D., 1992. Control of 40-Hz firing of reticular thalamic cells by neurotransmitters. Neuroscience 51, 259–268.
Robbins, T.W., 1997. Arousal systems and attentional processes. Biol. Psychol. 45, 57–71.
Schier, M.A., 2000. Changes in EEG alpha power during simulated driving: a demonstration. Int. J. Psychophysiol. 37, 155–162.
Schreckenberger, M., Langeasschenfeld, C., Lochmann, M., Mann, K., Siessmeier, T., Buchholz, H., Bartenstein, P., Grunder, G., 2004. The thalamus as the generator and modulator of EEG alpha rhythm: a combined PET/EEG study with lorazepam challenge in humans. Neuroimage 22, 637–644.
Sherman, S.M., Guillery, R.W., 1996. Functional organization of thalamocortical relays. J. Neurophysiol. 76, 1367–1395.
Sherman, S.M., Guillery, R.W., 2006. Exploring the thalamus and its role in cortical function. MIT Press, Cambridge, MA.
Steriade, M., 2000. Corticothalamic resonance, states of vigilance and mentation. Neuroscience 101, 243–276.
Swick, D., Pineda, J., Schacher, S., Foote, S., 1994. Locus coeruleus neuronal activity in awake monkeys: relationship to auditory P300-like potentials and spontaneous EEG. Exp. Brain Res. 101, 86–92.
Takahashi, N., Shinomiya, S., Mori, D., Tachibana, S., 1997. Frontal midline theta rhythm in young healthy adults. Clin. Electroencephalogr. 28, 49–54.
Thomas, M.L., Sing, H.C., Belenky, G., Holcomb, H.H., Mayberg, H.S., Dannals, R.F., Wagner, H.N., 2003. Neural basis of alertness and cognitive performance impairments during sleepiness: II. Effects of 48 and 72 h of sleep deprivation on waking human regional brain activity. Thalamus Relat. Syst. 2, 199–229.
Torsvall, L., aAkerstedt, T., 1987. Sleepiness on the job: continuously measured EEG changes in train drivers. Electroencephalogr. Clin. Neurophysiol. 66, 502–511.
Uchida, S., Maloney, T., March, J.D., Azari, R., Feinberg, I., 1991. Sigma (12–15 Hz) and Delta (0.3–3 Hz) EEG oscillate reciprocally within NREM sleep. Brain Res. Bull. 27, 93–96.